공학석사 학위논문

A Study on the Hull Form Optimization of Semi-submersible FPU Considering Seakeeping Capability and Structural Weight

운동성능과 구조중량을 고려한 반잠수식 FPU의 하부구조 형상최적화에 관한 연구

2014 년 2 월

서울대학교 대학원

조선해양공학과

박 용 만

A Study on the Hull Form Optimization of Semi-submersible FPU Considering Seakeeping Capability and Structural Weight

지도 교수 장 범 선

이 논문을 공학석사 학위논문으로 제출함
2014 년 2 월

서울대학교 대학원
조선해양공학과
박 용 만

박용만의 공학석사 학위논문을 인준함
2014 년 2 월

위 원 장 _____ (인)

부위원장 _____ (인)

위 원 _____ (인)

Abstract

A Study on the Hull Form Optimization of Semi-submersible FPU Considering Seakeeping Capability and Structural Weight

In this paper, the optimal hull form of the real semi-submersible FPU with the minimum vertical motion and the minimum structural weight is determined.

As the oil and gas fields in deep water is developed widely these days, the demand for floating type offshore units is increasing. The floating units are usually encountered with severe seas so that the large vertical motion occurs which can induce the operational downtime. Since avoiding the downtime leads to the economic advantage, semi-submersible type units which have relatively good seakeeping capability are being preferred.

The amplitude of wave-induced motion is closely related to the hull form. Therefore, it is necessary to determine the optimal hull form in order to maximize the advantage of floating type structures. In this paper, fully automated procedure for the optimization of semi-submersible FPU's hull form is introduced and optimization is

performed based on real model.

Commercial software DNV WADAM is used for motion analysis. In order to automatically generate two files which are needed for WADAM as input, three modules are developed.

In panel generation module, hull structure is divided into ten parts and ten geometric parameters which correspond to the dimension of each part are defined. B-spline surface is used for geometric representation. Mesh elements are generate in equal interval according to the global mesh size.

In mass estimation module, weight and vertical center of gravity of total structure are estimated. Mass element is divided into several part; topside, steel, outfit, ballast water and remaining. Estimation is based on geometric characteristics such as length, surface area and volume.

In conditions setting module, conditions for analysis like angular frequency, wave heading angle, sea state are set. In addition, 53 points for air gap analysis are defined in this module.

Simulated annealing algorithm is adopted for the optimization. Four design variables are used. Among ten geometric parameters, only three major dimensions are selected. Additional variable is

defined for flexible control of the amount of ballast water. As constraints, GM, minimum air gap, freeboard, draught, total hull height are considered. The distance between columns remains constant to support topside structures.

Two weighting factors which correspond to two objectives, minimizing heave response and minimizing structural weight, are applied. By alternating the value of the factors, four optimal solutions are found. As the preference for structural weight is increased, total hull height is shortened accordingly. But this leads to worse seakeeping capability. It is confirmed that total hull height is in inverse proportion to heave response.

Keywords: Semi-submersible FPU, B-spline surface, heave response, structural weight, hull form optimization, simulated annealing

Student Number: 2011-23462

Contents

A Study on the Hull Form Optimization of Semi-submersible FPU Considering Seakeeping Capability and Structural Weight

List of Figures

List of Tables

1. Introduction

1.1. Background

As the oil and gas development field goes toward deeper locations, demands on floating type units are increasing compared to fixed type units. These floating units are usually encountered with severe seas so that large vertical motion occurs which can induce the operational downtime. Avoiding the downtime yields economic advantage from an operational point of view (OPEX). For this reason, semi-submersible type structures, shown in Fig. 1, are preferred because of the smaller water plane area which leads to smaller vertical motion.

Fig. 1 – Examples of semi-submersible units

The amplitude of wave-induced motion is closely related with hull form of floating structures. Thus, in order to maximize the advantage of adopting semi-submersible type units, it is important to determine the optimal hull form in early design stage.

Seakeeping capability is usually obtained by the model test or the numerical analysis. To find the best hull form which has the minimum vertical motion amplitude, a great number of model tests or the cumbersome jobs of manually varying dimensions for analysis should be performed. But those jobs are too time-consuming and expensive. So it is necessary to develop a fully automated numerical procedure for the hull form optimization.

In addition to seakeeping capability, structural weight is also an important factor in design of semi-submersible. It leads to both economic and environmental advantages. In general, the lighter hull structure weighs becomes, the cheaper construction cost becomes. Furthermore, the weight lightening can reduce the carbon emission of carrier vessel during the transport. In order to consider both performances, multi-objective optimization needs to be performed.

1.2. Previous Studies

There are plenty of studies on the hull form optimization of semi-submersible unit. However, most of them are in common actually. In this section, two representatives of the previous studies are introduced.

S. Akagi and K. Ito(1984) optimized the heave motion of semi-Rig [1]. Fig. 2 shows the structure used in Akagi's study. The adopted structure has the simplified geometry with cylindrical pontoons and cylindrical columns.

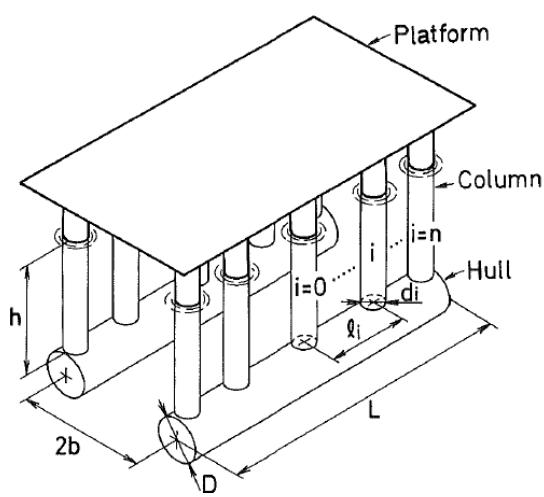

Fig. 2 – Semi-Rig structure adopted in Akagi's study

According to the number of columns, the diameters of hull and the longitudinal position of columns, the heave response spectrum is formulated analytically. Using quadratic programming method, the area of the spectrum is minimized. The natural frequency of heave motion was constrained to be less than the lowest value of wave spectrum to avoid the large response. BM is constrained as a stability condition.

Akagi and Ito(1984) also introduced the concept of multi-objective optimization [2]. Three objectives are considered: minimize the displacement, maximize the loading weight and minimize the heave response. Each objective is in the interest of minimizing the rate of operation respectively. As a result, three-dimensional Pareto set is obtained.

J. Lee and G. Clauss(2007) introduced fully automated numerical procedure for the optimization. The objective is to minimize the downtime of semi-FPU [3]. As shown in Fig. 3, the adopted model is not that simple but relatively realistic. NURB surface is used for geometric representation and the commercial software WAMIT is used for hydrodynamic analysis.

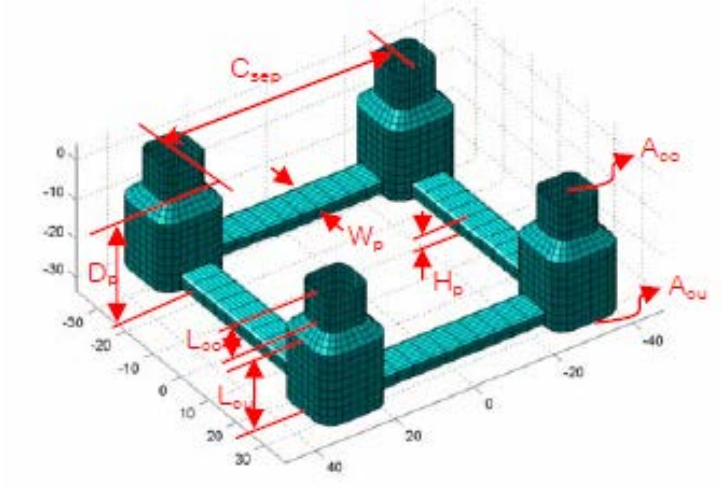

Fig. 3 – Semi-FPU structure adopted in Lee's study

Simulated annealing is used as an optimization algorithm. GM is constrained to be greater than 1.0m in order to consider stability. Regardless of the hull form, total weight remains fixed during the optimization process.

1.3. Summary on This Study

In this study, much more realistic semi-submersible FPU model is adopted. Fig. 4-(a) shows the real model in the drawing and 4-(b) shows the model generated in this study. It can be found that the details of real hull form, e.g. transition of the column corner radius, are well represented. For the geometric representation, B-spline and Bezier surface is used. For the hydrodynamic analysis, commercial software DNV.WADAM is used.

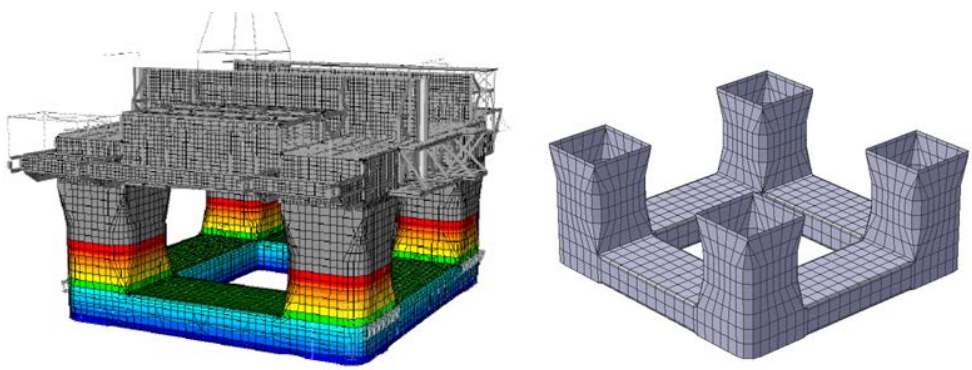

(a) (b)

Fig. 4 - Semi-FPU structure adopted in this study

In the optimization, two objectives are considered: to minimize heave motion and to minimize steel weight. Unlike Lee's study, the weight is not a constant so that it is also one factor to be optimized.

To calculate the ballast weight which is necessary for total weight and GM calculation, not only geometric parameters but also ballast water filling ratio is selected as a design variable.

Like previous studies, GM and freeboard are considered as the constraints for stability and loading capacity. Air gap is also considered as an additional constraint. The air gap is the distance between the water surface and the deck and it varies by the relative motion between wave elevation and vertical displacement of the structure. With negative air gap, the bottom slamming may happen at the topside structure. To avoid this risk, air gap should be considered.

Fig. 5 shows the schematic procedure of the optimization used in this study. First, the optimizer – simulated annealing algorithm is used in this study – sets the values of design variables. Three modules are introduced to generate input files for the motion analyzer, WADAM. For hydrodynamic analysis, WADAM needs two input files. One contains the nodal and elemental information of panel meshes, the other contains the conditions of hydrodynamic analysis. Those two files are generated automatically by three modules. When short term analysis is done, the optimizer evaluates

the constraints and the objective values. Until the optimizer meets the convergence criteria, the process mentioned above is iterated continuously.

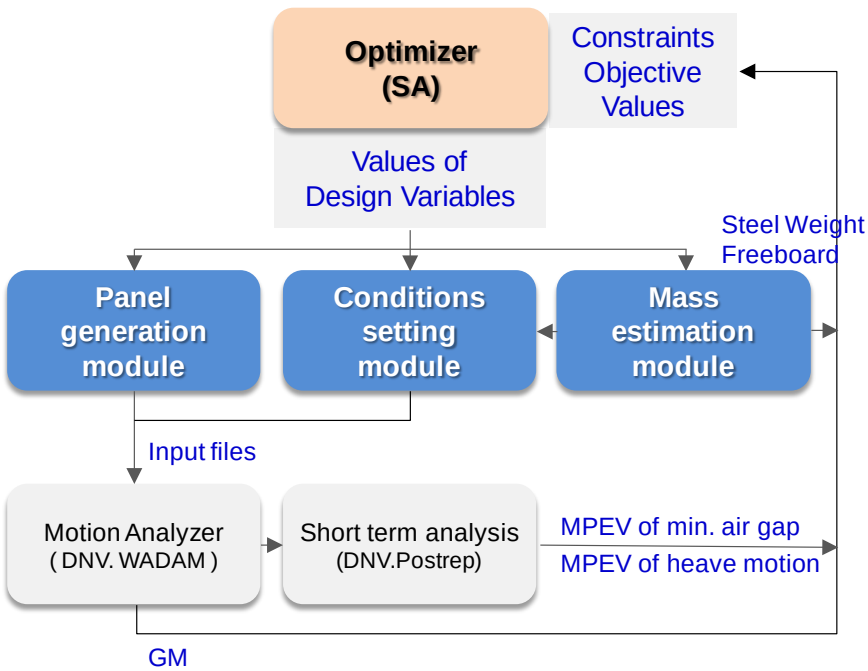

Fig. 5 – Schematic procedure of the optimization used in this study

Three modules are the key part of this study. The details of them will be handled in the latter section. After that, the details of the optimization will be explained.

2. Modules for Optimization

2.1. Panel Generation Module

2.1.1. Model Division

This module generates the panel mesh file which is one of input files for WADAM. In order to generate mesh, hull geometry needs to be defined first. For simplified geometric representation of complicated hull form, total model is divided into ten parts as shown in Fig. 6.

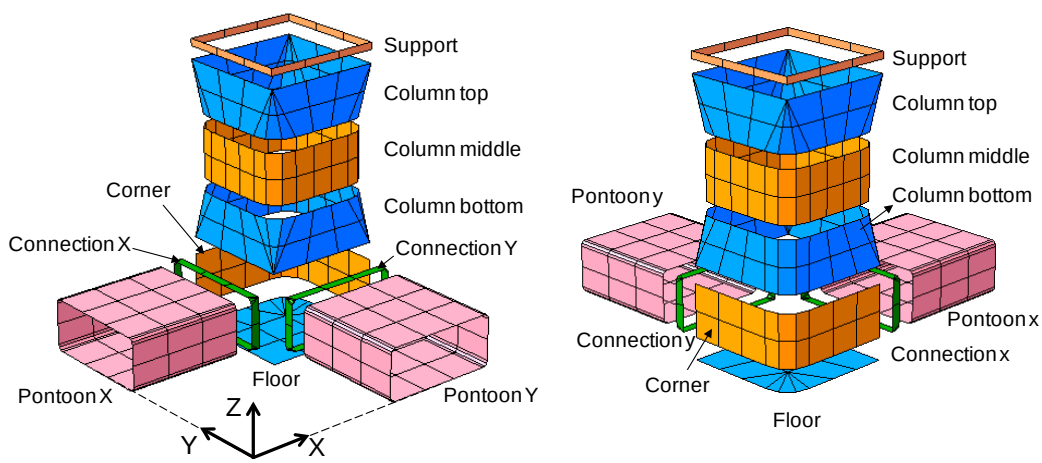

Fig. 6 – Model division into ten parts

Since the model is symmetric to XZ and YZ plane, only quarter model is used. The division is based on whether the corner radius

increases, decreases or remains constant along the longitudinal direction. Although connection and support are transition parts which rarely affect the seakeeping capability, they are also considered to represent sophisticated hull form which is almost same as the drawings.

2.1.2. Geometric Parameter Definition

Total ten independent parameters are introduced to represent the predefined ten parts. Each parameter corresponds to dimension of the parts. Fig. 7 indicates the parameters and Table 1 describes the definition of parameters.

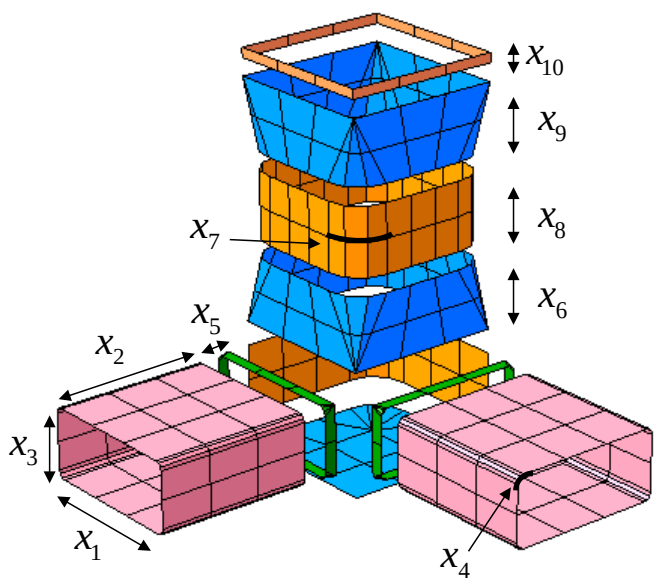

Fig. 7 – Definition of ten geometric parameters

Table 1 – Definition of ten geometric parameters

Parameter	Definition
x1	Width of 'Pontoon' parts
x2	Length of 'Pontoon' parts
x3	Height of 'Pontoon' parts
x4	Corner radius of 'Pontoon' parts
x5	Length of 'Connection' parts
x6	Length of 'Column bottom' part
x7	Corner radius of 'Column' parts
x8	Length of 'Column middle' part
x9	Length of 'Column top' part
x10	Length of 'Support' part

These parameters are able to represent hull main dimension and also able to represent the transition of corner radius so that the geometric continuity is achieved.

2.1.3. Geometry Definition

Geometric information of ten predefined parts are defined independently by Bezier & B-spline method. For all parts, one surface is composed of sectional curves and one curve is composed of points. Points on surface are defined by parameters u and w, which indicate the relative position of points in longitudinal and circumferential direction respectively. The location of each section is determined by parameter u which varies from 0 to 1 and the location of points on each section is determined by parameter w. Regardless of the sectional shape, same point distribution can be obtained by same value of parameter w. This is the big advantage of using B-spline method and the essential characteristic to generate iso-mesh. Fig. 8 shows how points on surface are distributed by two parameters.

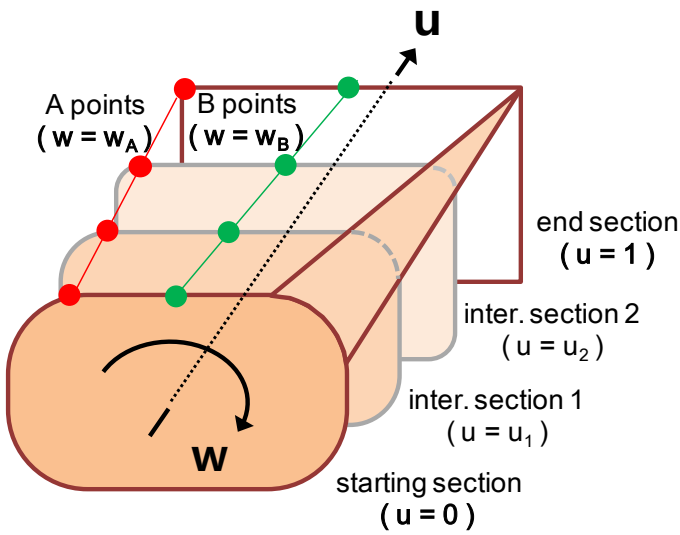

Fig. 8 – Point distribution determined by two parameters

As an example, four sections are shown in the Fig.. Although each section has different corner radius, A points which are located at the end of corner correspond to the same value of parameter w (w_A). Likewise B points which are located at the middle of upper side correspond to the same value of parameter w (w_B).

Bezier & B-spline method is also flexible to express corner curvature by distributing control points at the appropriate positions. Furthermore, asymmetric corner in a section and varying corner curvature can be modeled easily. Asymmetric corner stands for the corner whose radius is different to radius of others. Fig. 9 shows an example of asymmetric corner.

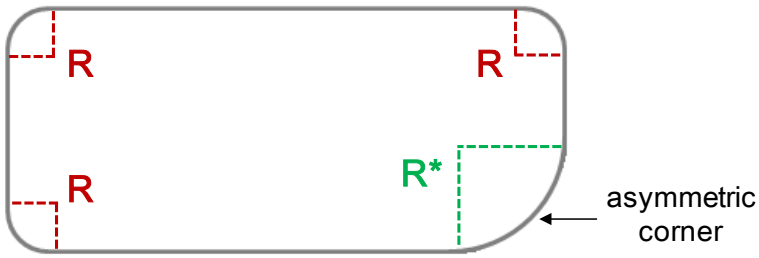

Fig. 9 – Asymmetric corner

Total 36 (18×2) control points are used to define one section. In order to represent the closed curve, 18 control points are used at the starting and end section respectively. According to the dimension of the part, the position of control points is determined. To define closed section, some control points are to be overlapped at the same position. Fig. 10 shows the arrangement of control points in a part.

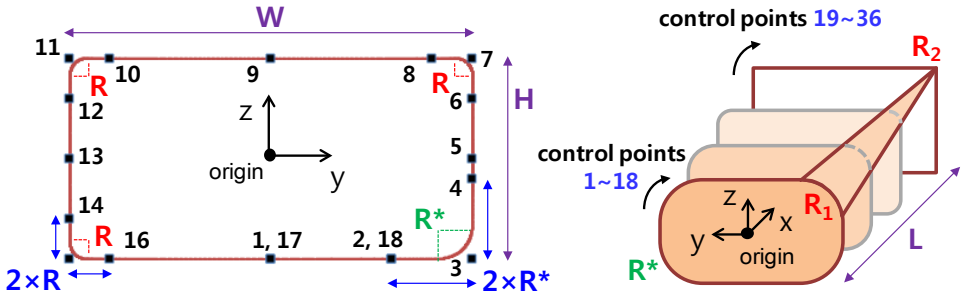

Fig. 10 – Arrangement of 36 control points to define one part

Initially, the origin of every part is supposed to be (0, 0, 0) and the surface progresses toward x−axis. But every surface has its designated position and direction of progress as shown in Fig. 6. So control points should be rotated and translated after arrangement. Rotation of the control points is performed by mapping method shown in Fig. 11. Translation can be done simply by adding the coordinate of designated origin to the coordinate of every control points.

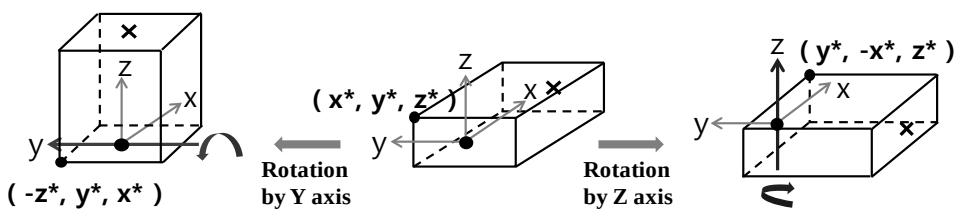

Fig. 11 − The method of mapping to rotate control points

Geometry of each part is defined by the formula (1) ~ (5).

$$Q(u,w)=\sum_{i=0}^{1}\sum_{j=1}^{18}B_{i,j}J_i^1(u)K_j^3(w) \qquad (1)$$

$$J_i^1(u)=u^i(1-u)^{1-i} \qquad (2)$$

$$K_j^k(w) = \frac{(w - y_j)K_j^{k-1}(w)}{y_{j+k-1} - y_j} + \frac{(y_{j+k} - w)K_{j+1}^{k-1}(w)}{y_{j+k} - y_{j+1}} \quad (3)$$

$$K_j^1(w) = \begin{cases} 1 & \text{if } y_j \le w \le y_{j+1} \\ 0 & \text{otherwise} \end{cases} \quad (4)$$

$$y_l = l - 1 \qquad (1 \le l \le 21) \quad (5)$$

The mathematical definition of the surface is described in (1). $B_{i,j}$ corresponds to 36 control points and $J_i^1(u)$, $K_j^3(w)$ corresponds to basis function of Bezier and B-spline curve respectively. The index i can have values of 0 and 1 which indicates starting section and end section. The index j can have integer values from 1 to 18 and each of value indicates the control points in a section.

The basis function of 1st order Bezier curve is described in (2). This function linearly interpolates control points between starting section and end section by the parameter u. As shown in (3), the basis function of B-spline curve is obtained by the recursive formula. In this study, B-spline curve of degree 3 is used, which needs three adjacent control points to represent curve segment.

Corner radius is also represented by three control points at the corner and defined as half of the interval between three adjacent control points at the corner. In regard to this characteristic, there needs to be a constraint for sectional dimension, such that twice of corner radius should be not more than half of width(W) and height(H). This can be written in mathematical from like (6).

$$R \leq \min(0.25H,\ 0.25W) \tag{6}$$

2.1.4. Mesh Generation

Mesh generation is performed for ten parts independently. According to the global mesh size which is chosen by designer, the number of elements in three direction is determined as shown in Fig. 12.

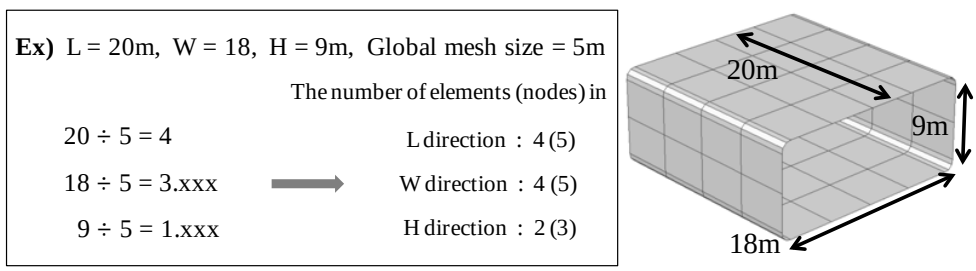

Fig. 12 – The method to determine the number of elements in one part

Fig. 13 shows the procedure of node generation. In the starting and end section, nodes are generated at the end of corners. Dividing length(L), width(W) and height(H) into the number of elements in each direction, nodes are generated in equal interval. At the section whose corner is not the right angle, two additional nodes are generated in the corner. Elements are generated by connecting adjacent nodes.

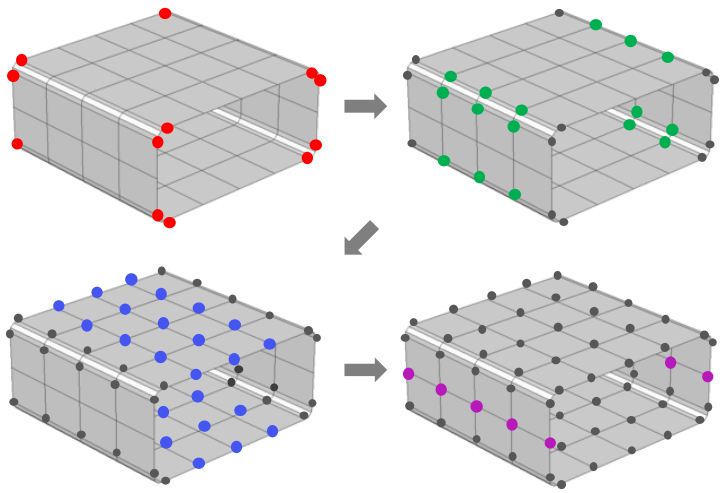

Fig. 13 – The method to generate nodes and elements in one part

Unlike elements in other parts are located on the circumferential surface, elements in the floor part are located inside the flat surface. So another method which is shown in Fig. 14 is introduced to generate elements in the floor part.

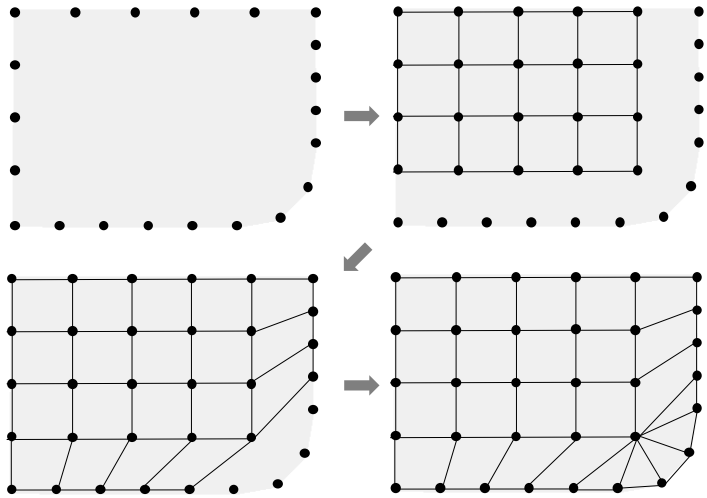

Fig. 14 – The method to generate nodes and elements in the floor part

First nodes are generated along the boundary curve in accordance with global mesh size. Additional nodes are generated in parallel with external nodes and rectangular meshes are generated. After that quadrangular meshes are generated at side of the surface. Finally triangular meshes are added by connecting remaining adjacent nodes.

2.2. Mass Estimation Module

2.2.1. Weight Estimation

During the optimization process, hull form is changed continuously. If hull form is changed, mass information should be also modified. In this module, weight and center of gravity of arbitrary hull form is estimated. Then corresponding draught is calculated. Among all things, weight estimation should be performed first because others are calculated based on weight.

It is obvious that a lot of mass data is needed for accurate estimation. But in most offshore companies, the mass data is kept confidential. In this study, data from three semi-FPUs is used.

Total weight is divided into five elements.

- topside weight
- hull steel weight
- hull outfit weight
- ballast water weight
- remaining

Each element is estimated based on surface area, volume and height of the hull structure. For simple calculation of the surface area and the volume, hull shape is simplified to be rectangular as shown in Fig. 15.

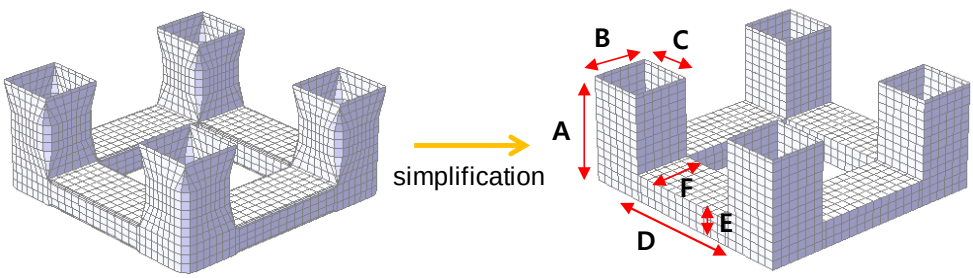

Fig. 15 – Rectangular simplification of hull shape

Using the dimensions in Fig. 15, surface area and volume is calculated by the formula (7) ~ (9). Because of the symmetry, only one column and one pontoon are considered.

$$\text{Hull Surface Area } (\text{m}^2) = (2A - E)(B + C) + BC + 2D(E + F) \quad (7)$$

$$\text{Hull Volume } (\text{m}^3) = ABC + DEF \quad (8)$$

$$\text{Pontoon Volume } (\text{m}^3) = BCE + DEF \quad (9)$$

In general, capacity and weight of the topside is fixed in the early design stage. So topside weight is not relevant to hull form and remains constant during the optimization process.

Hull steel weight is assumed to be proportional to the hull surface area. The portion of inner stiffeners in total steel weight is much smaller than that of outer plates. Moreover, the variance of plate thickness is negligible. So it is not against common sense that hull surface area is the dominant factor of hull steel weight and they are in proportional relation.

Table 2 – Relation between hull steel weight and hull surface area

Model	Hull steel weight (ton)	Surface area (m^2)	Proportional constant (ton/m^2)
1	27933	9171	3.05
2	19000	5059	3.76
3	35434	9586	3.81
		Average	3.54

Table 2 shows how the proportional constant between hull steel weight and hull surface area is obtained. The proportional constants calculated from three real semi-FPUs are averaged. As a result, it

is found that hull steel weight is calculated by multiplying hull surface area by 3.54. The difference between the averaged valued and the value of each model is within 15%. It can be regarded for the averaged value to be quite reliable. The mathematical form to calculated hull steel weight is like (10).

$$\text{Hull Steel Weight (ton)} = 3.54 \times \text{Hull Surface Area} \quad (10)$$

Table 3 – Relation between hull outfit weight and hull volume

Model	Hull outfit weight (ton)	Volume (m^3)	Proportional constant (ton/m^3)
1	5000	46354	0.1076
~~2~~	~~13000~~	~~18926~~	~~0.6868~~
3	6066	52137	0.1163
		Average	**0.1121**

Hull outfit weight is assumed to be proportional to the hull volume. Table 3 shows how the proportional constants between hull outfit weight and hull volume is obtained. The proportional constants calculated from two real semi-FPUs are averaged. Due to severe discordance of tendency on weight and volume, data of the second model is excluded for averaging. As a result, it is found that

hull outfit weight is calculated by multiplying hull volume by 0.1121. The difference between the averaged valued and the value of two models is within 5%. The mathematical form to calculated hull steel weight is like (11).

$$\text{Hull Outfit Weight (ton)} = 0.1121 \times \text{Hull Volume} \quad (11)$$

Even if the hull form is same, total weight and center of gravity can be totally different according to the amount of ballast water. So the amount of ballast water should also be considered as changeable and independent element regardless of hull form. For this reason, ballast filling ratio which corresponds to the ratio of volume of ballast water to volume of pontoon is introduced as a design variable of the optimization. Then the volume of ballast water can be calculated by multiplying the pontoon volume by ballast filling ratio and ballast water weight is calculated by multiplying the ballast volume by seawater density. This can be written in mathematical form like (12).

$$\text{Ballast Water Weight (ton)} = 1.025 \times \text{Pontoon Volume} \times \text{Ballast filling ratio} \quad (12)$$

Remaining element consists of design margin, fresh water, fuel, marine load and regression error. Regression error is due to the difference between averaged proportional constant and that of reference model. These sub-elements are assumed not to be relative with hull form. So remaining element remains constant during the optimization.

Table 4 shows the summary of the weight estimation method.

Table 4 – Summary of the weight estimation method

Element	Estimation
Topside weight	constant
Hull steel weight	3.54 × hull surface area
Hull outfit weight	0.1121 × hull volume
Ballast water weight	1.025 × pontoon volume × ballast filling ratio
Remaining	constant

2.2.2. Center of Gravity (CoG) Estimation

Because of the symmetry, X and Y coordinate of the center of gravity is zero. Similar to the weight estimation, the vertical center of gravity(VCG), Z coordinate of CoG, is divided into four elements.

- topside VCG
- hull lightweight VCG
- ballast water VCG
- remaining

For the same reason with the weight of topside, VCG of topside itself also remains constant during the optimization. In order to calculate VCG of whole structure including both topside and hull, height of hull is added to VCG of topside itself.

Unlike steel weight and outfit weight are considered separately, they are combined as hull lightweight in VCG estimation. Based on the assumption that density of outer plates is uniform, VCG of hull lightweight can be regarded as the center of area of outer plates. Using the dimensions shown in Fig. 15, this is calculated by the formula (13).

$$\text{Hull LWT VCG} = \frac{A^2(B+C)}{2} + (A-E)(B+C)\left(E + \frac{A-E}{2}\right) + E^2 D + DEF \quad (13)$$

Although tanks for ballast water are located at both pontoon and column, it is common that tanks in column are empty and tanks in pontoon are only used. So ballast water VCG is considered to be half of pontoon height.

VCG of remaining element is assumed to be proportional to hull height. The proportional constant is 0.4 and this constant is determined by adjusting total VCG to be identical with the reference value.

Table 5 shows the summary of the VCG estimation method.

Table 5 – Summary of the VCG estimation method

Element	Estimation
Topside VCG	constant
Hull lightweight VCG	center of area of outer plates
Ballast water VCG	half of pontoon height
Remaining	0.4 × hull height

2.2.3. Draught Calculation

In the weight estimation process, the simplified rectangular model is used to calculate the structural volume. However if the difference between displaced volume and total weight is too large, WADAM doesn't initiate the analysis. So the curvature of corners should be also considered for precise draught calculation. As shown in Fig. 16 and formula (14) ~ (18), the volume of one part is calculated by integrating sectional areas and the area of each section is calculated by dividing into four segments.

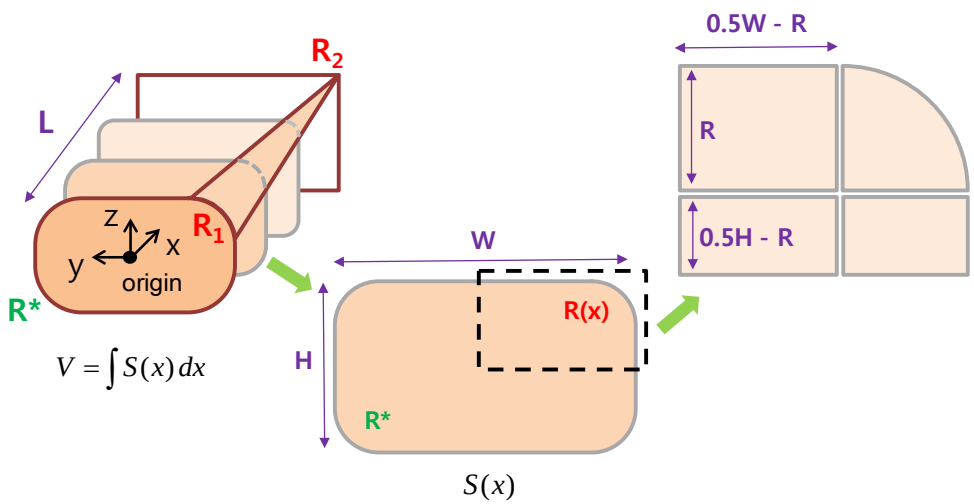

Fig. 16 – Segment division to calculate the volume of one part

$$S_{1/4} = \frac{WH}{4} - R(x)^2 \left(1 - \frac{\pi}{4}\right) \tag{14}$$

$$R(x) = \frac{R_2 - R_1}{L} x + R_1 \tag{16}$$

$$V_{1/4} = \int_0^L S(x)\, dx = \frac{WHL}{4} - \left(1 - \frac{\pi}{4}\right)\left(\frac{a^2 L^3}{3} + aR_1 L^2 + R_1^2 L\right) \tag{17}$$

$$a = \frac{R_2 - R_1}{L} \tag{18}$$

After calculating the volume of every parts, the part at which free surface is located is indentified first. Then, the expected position of free surface which is calculated roughly by assuming that the part is rectangular. From that position, draught is kept changing by 0.0001m until the difference between displaced volume and total weight is less than 1%.

2.3. Conditions Setting Module

2.3.1. Conditions for Motion Analysis

To find the optimal solution, very large number of analyses is necessary. The aim of optimization is not a quantitative analysis but a qualitative comparison. So it is important not to set up analysis conditions too excessive. Table 6 shows the conditions for motion analysis used in this study.

Table 6 – Conditions for motion analysis

Conditions	Contents
Frequency range	0.1 ~ 1.3 rad/sec
Heading angle	0° , 45°
Heave damping	4% of critical damping
Water depth	300 m
Wave spectrum	Pierson-Moskowitz spectrum
Sea state	H_s = 14.69m, T_z = 11.06s

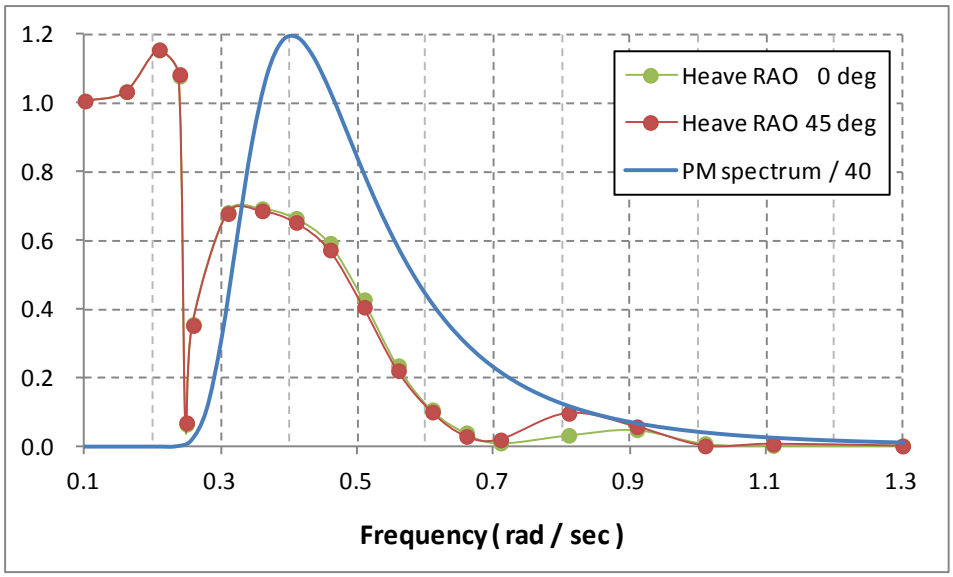

Fig. 17 – Sampling of 20 points of frequency for motion analysis

As shown in Fig. 17, 20 points of frequency are sampled in the interval between 0.1 rad/sec and 1.3 rad/sec. In the interval from 0.3 rad/sec to 0.7 rad/sec, the distance between frequencies are narrower than other intervals. In that interval, the wave spectrum is meaningful while the spectrum is nearly

To perform a short term analysis, Pierson–Moskowitz spectrum, defined by significant wave height H_s and zero up–crossing period T_z, is used. In this study, 14.69m of H_s and 11.06s of T_z are used. This sea state corresponds to 1000–year return period of the reference location.

2.3.2 Conditions for Air gap Analysis

The procedure of air gap analysis used in this study is like below.

1. Calculate the sea surface elevation at the designated points which are located on the free surface.
2. Define specific points on the structure for which the air gap is to be analyzed. These points are above the points at which the sea surface elevation is known.
3. Define the absolute displacement of specific points in vertical direction. Define the transfer function as the difference between the absolute displacement of specific points and the sea surface elevation below.
4. Air gap = Freeboard − 1.2 × Short term value.

The procedure above is described in Fig. 18, 19.

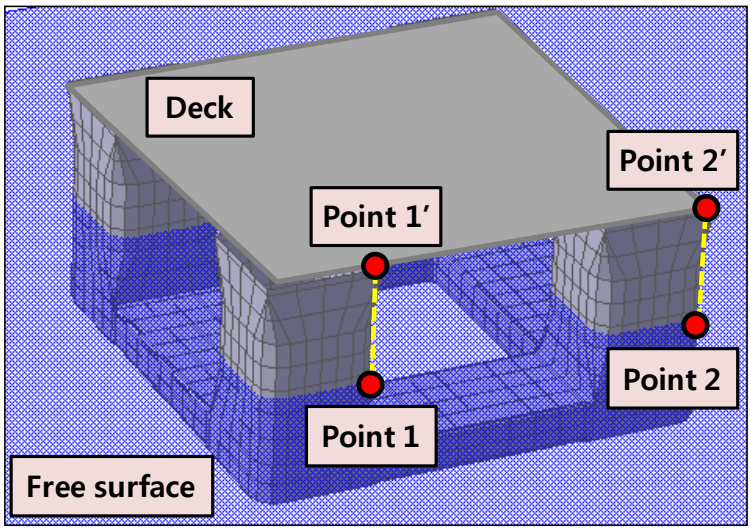

Fig. 18 – Points of free surface and corresponding points of deck

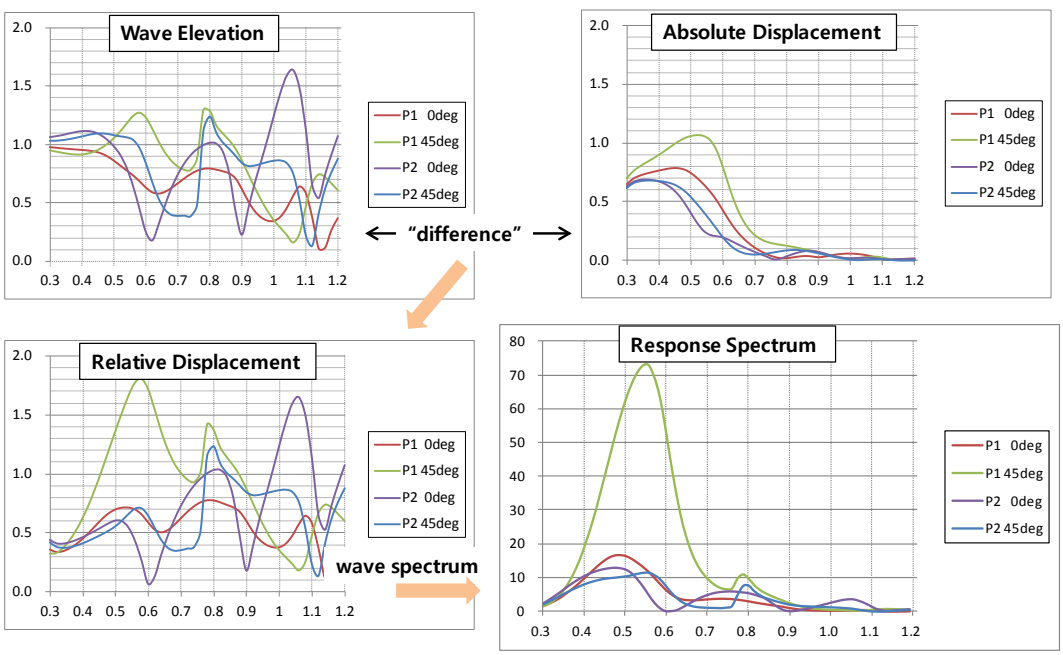

Fig. 19 – Procedure to calculate the spectrum of relative motion

Total 53 points are selected for air gap analysis and the horizontal location of points are shown in Fig. 20.

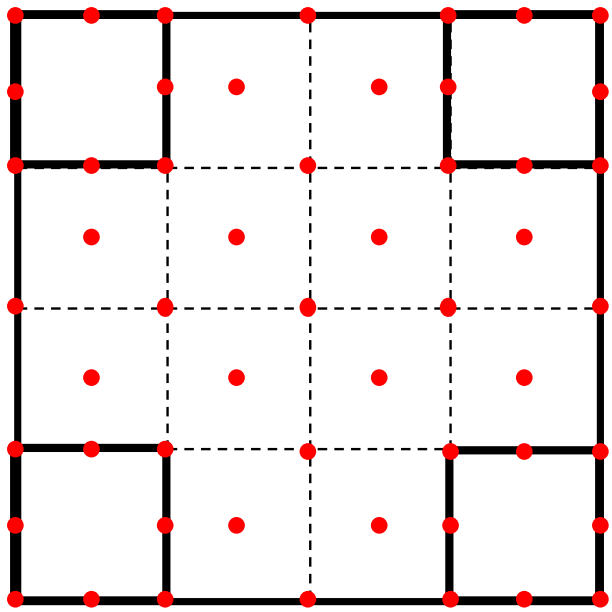

Fig. 20 – Horizontal position of 53 points for air gap analysis

3. Optimization

3.1. Simulated Annealing

In this study, simulated annealing is adopted as the optimization algorithm. This algorithm is a kind of probabilistic search method which is widely used for global optimization problems with several local minima.

The name and concept of this algorithm come from the physical process that a metal is slowly cooled until the structure is frozen at a minimum energy state. So the 'temperature' and the 'energy', even if they do not correspond to the very physical quantity, represent each design point. In general, the temperature is decided by the iteration number and the energy is decided by the value of objective function.

The algorithm takes random moves through the design space, looking for points with low energies. In these random moves, the probability of taking new point is determined by the Boltzmann distribution. If the new energy is lower, transition of the design point will occur. If the new energy is higher, the transition still can

occur depending on the probability which is determined by the energy difference and the temperature. This probability of taking new point with higher energy is what allows simulated annealing to get out of local minima. The temperature is initially set to a high value and is lowered with the iteration proceeds.

To finish the iteration, the convergence criteria is needed. The number of iteration and the change of objective function are usually used. But there are no such standard of criteria, so criteria setting is quite difficult. In this study, the number of iteration is fixed as 400 times. Four design variables are used in the optimization, and the details of these variables shall be explained in latter section. In one iteration step, four variables are altered gradually so that total 1600 design points are to be checked. Fig. 21 shows the flow of simulated annealing algorithm of each 200 times iteration and Table 7 shows the conditions of the algorithm.

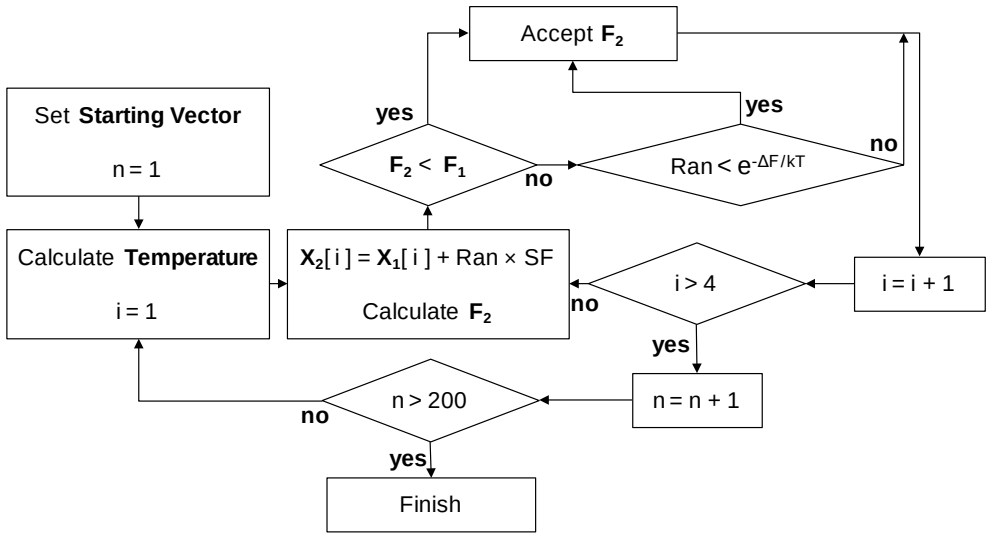

Fig. 21 – Flowchart of simulated annealing algorithm

Table 7 – Conditions of the simulated annealing algorithm

Conditions	Contents
Number of design variables	4
Convergence criteria	n = 200(× 2)
Scale factor	1.0, 0.01
Boltzmann constant	k =1
Starting point	Random setting
Temperature	$T = 300 \times 0.98^{n}$

For the first 200 times, the variation between two points is

relatively large for a wide search. On the other hand, for the last 200 times, the variation is relatively small for a detailed search. These variation is controlled by the scale factor.

The code of simulated annealing is developed by the author. To verify the code, Goldstein & Price function which has several local minima is used. The function is often used for validation of global minimization problem and is mathematically defined like (19).

$$f_{gold} = \left[1+\left(x_1+x_2+1\right)^2 \cdot \left(19-14x_1+2x_1^{\,2}-14x_2+6x_1x_2+3x_2^{\,2}\right)\right] \cdot \left[30+\left(2x_1-3x_2\right)^2 \cdot \left(18-32x_1+12x_1^{\,2}+48x_2-36x_1x_2+27x_2^{\,2}\right)\right] + x_3^{\,2}+x_4^{\,2} \qquad \left(\text{subject to } -2 \le x_i \le 2\right) \tag{19}$$

The last two terms which are marked red are intentionally introduced to validated the code for the problem with four design variables. To minimize the function, the additional variables, x_3 and x_4, must be zero. The shape of the original function without x_3 and x_4 is shown in Fig. 22.

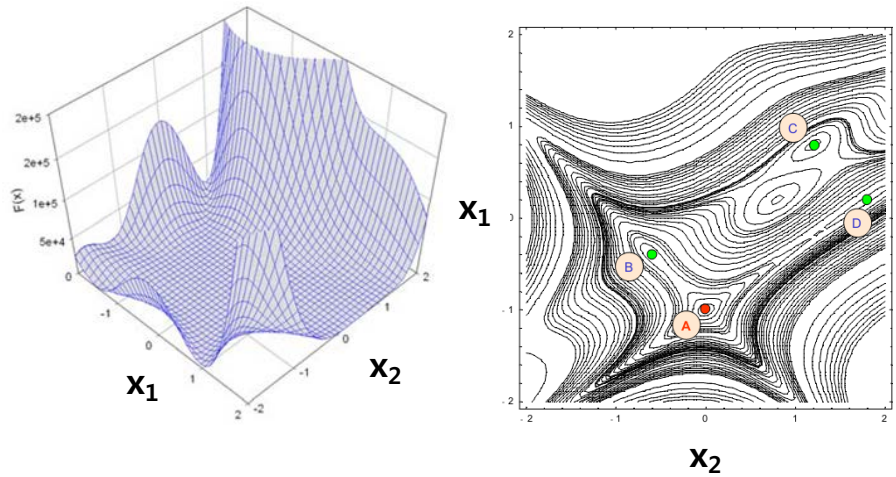

A : Global minimum (0.0, -1.0) f = 3.0
B : Local minimum (-0.6, -0.4) f = 30.0
C : Local minimum (1.2, 0.8) f = 840.0
D : Local minimum (1.8, 0.2) f = 84.0

Fig. 22 – Goldstein–Price function

Table 8 – The global minimum of Goldstein–Price function by SA

Try	Starting point				Result				
	x_1	x_2	x_3	x_4	x_1	x_2	x_3	x_4	f
1st	−0.55	−0.17	−1.32	−1.56	0.01	−0.99	0.00	0.00	**3.03**
2nd	0.44	0.33	−0.92	−1.71	0.00	−1.00	0.00	0.01	**3.01**
3rd	1.04	−0.72	0.85	0.28	0.00	−1.00	−0.01	0.00	**3.00**
4th	1.18	0.78	1.95	−0.62	0.00	−1.00	−0.01	0.00	**3.01**
5th	0.00	0.00	0.00	0.00	0.00	−0.99	0.00	0.01	**3.02**

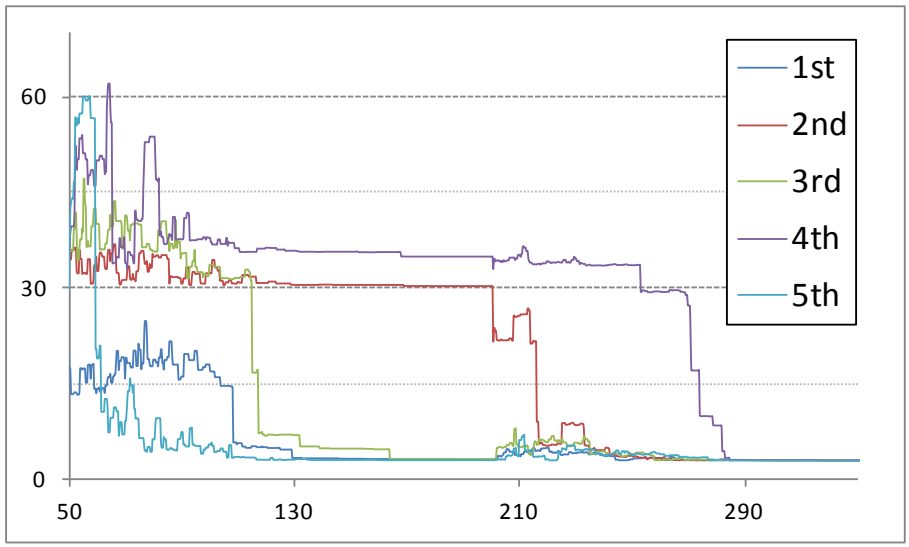

Fig. 23 – The global minimum of Goldstein–Price function by SA

From the five different starting points, simulated annealing is adopted to minimize Goldstein–Price function. Regardless of the starting point, the code well leads design points to the global minimum. Table 8 and Fig. 23 show this result.

3.2 Design Variables

In the panel generation module, total ten geometric parameters are already defined. But not all of parameter are critical to both seakeeping capability and structural weight. It can be thought that the important factor to those performances is the main dimension of whole hull structure. The partial dimension of each component and the corner radius have relatively less importance. Moreover, much more time is to be spent for the optimization in proportional to the number of design variables. For efficient optimization, total three design variables which represent the hull form are newly defined by combining ten geometric parameters. These new variables correspond to the column width, the column height and the pontoon height. Fig. 24 shows three design variables for hull form representation.

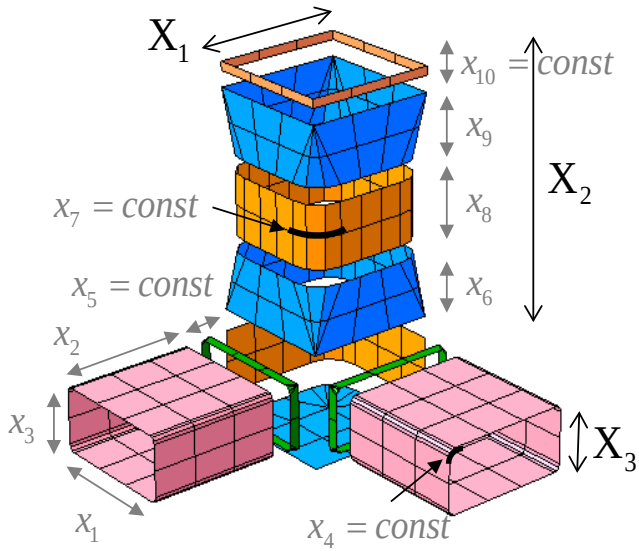

Fig. 24 – Three geometric design variables

To distinguish form the geometric parameters, new design variables are written in the capital letters. The design variables X_1 ~ X_3 are connected with geometric parameters $x_1 \sim x_{10}$ like (20) ~ (27). Some minor parameters are fixed as constant.

$$X_1 = x_1 \qquad (25.0 \le X_1 \le 34.65) \tag{20}$$

$$X_2 = x_6 + x_8 + x_9 + x_{10} \qquad (25.29 \le X_2 \le 46.96) \tag{21}$$

$$X_3 = x_3 \qquad (8.31 \le X_3 \le 15.44) \tag{22}$$

$$x_4 = \text{constant} = 1.25m \tag{23}$$

$$x_5 = \text{constant} = 2.0m \quad (24)$$

$$x_7 = \text{constant} = 6.2m \quad (25)$$

$$x_{10} = \text{constant} = 1.625m \quad (26)$$

$$x_6 : x_8 : x_9 = 3:4:3 \quad (27)$$

To prevent the immoderate change and the geometric unbalance, the hull form variables, X_1 ~ X_3, are bounded form −30 percent to 30 percent of the reference value. Table 9 shows the reference value and the upper/lower bound of three variables. Though the reference value is supposed to be 18.66, it is modified to 25.0 because of (6) and (25).

Table 9 − Upper & lower bound of geometric design variables

Design Variable	−30%	Reference	+30%
X_1	18.66	26.65	34.65
X_2	25.29	36.125	46.96
X_3	8.31	11.875	15.44

As mentioned in 2.2.1, the ratio of the amount of ballast water to the pontoon volume is also defined as a design variable. Ballast

filling ratio is written as X_4 and is express in decimal form which corresponds to the percentage.

$$0.0 \le X_4 \le 0.75 \tag{28}$$

The ballast filling ratio, X_4, is up to 75% as shown in (28). The rest 10% is for pump and motor room, another 10% is for adjusting trim and heel, the other 5% is compensation for the error that is due to the rectangular simplification of pontoon corner.

3.3 Objectives and Constraints

There are two objectives of the optimization.

- Minimize 3-hour heave MPEV
- Minimize hull steel weight

Among the vertical motions, only heave motion is selected as the objective. That's because heave is the dominant motion compared to pitch and roll. As shown in Fig. 22, the scale of heave motion RAO is 100 times larger than pitch motion RAO. The magnitude of heave response of 0 degree is larger than the response of 45 degree. This also can be found by the RAO shown in Fig. 25.

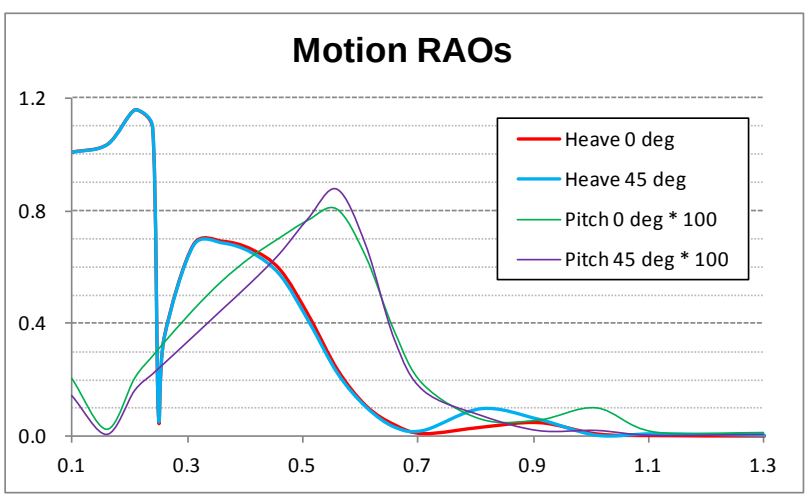

Fig. 25 – Comparison between the scale of heave and pitch RAOs

Two objectives are combined into one function by introducing the weighting factors like (29).

$$\phi = W_{Heave}\left[\frac{\text{Heave } 0^\circ}{\text{Ref. Heave } (6.75\text{m})}\right] + W_{Weight}\left[\frac{\text{Hull Steel Weight}}{\text{Ref. Steel Weight } (33945\text{ton})}\right] \quad (29)$$

The constraints are set up like below.

- $\text{GM} \geq 8.0\text{m}$
- $\text{min. Air gap} \geq 2.0\text{m}$
- $\text{Draught} \geq \text{pontoon height}$
- $\text{Freeboard} \geq \text{min. Air gap} + \frac{H_{\max}}{2}\left(2.0 + \frac{2\times 14.69}{2} = 16.69\text{m}\right)$
- $\text{Total hull height} \leq 55.2\text{m}\,(15\%\ \text{increase from the reference})$
- $\text{Distance between column centers remains constant}\ (83.65\text{m})$

GM and the minimum air gap are forced to be better than each value of the reference model, 7.98m and −0.06m respectively. If the displacement is either too large or too small so that the draught is off the column, the optimizer moves to next design point without motion analysis. The increase of total hull height is forced not over

15% of the reference model. There might be problems of construction if the hull height is too large. Problems in transport also can occur because of the high VCG. The distance between column centers is kept identical with the reference value because the size of topside is fixed.

3.4 Results

As a result of the optimization, four optimal solutions are obtained. Each solution corresponds to the different weight factors. Fig. 26 shows the two-dimensional Pareto set and Table 10 shows the value of two objectives corresponding weighting factors.

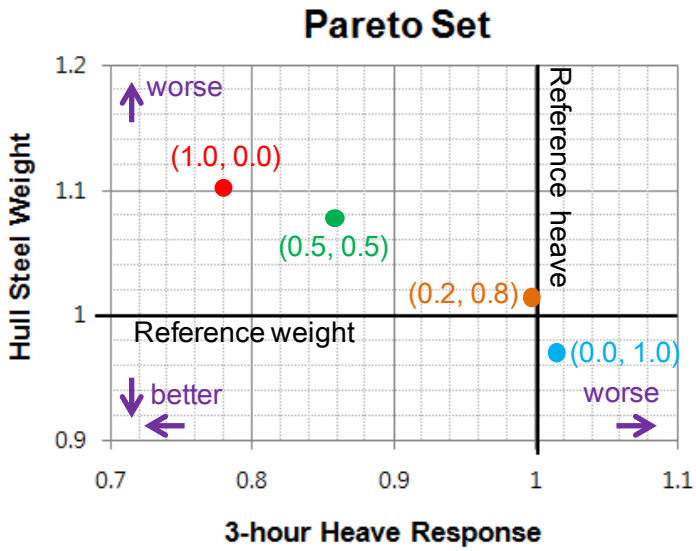

Fig. 26 – Pareto optimal solution set of the optimization

Table 10 – Objectives of the optimal solutions

W_{Heave}	W_{Weight}	Heave 0 °	Steel Weight
1.0	0.0	5.25m (0.78)	37412ton (1.10)
0.5	0.5	5.78m (0.86)	36642ton (1.08)
0.2	0.8	6.74m (0.99)	34414ton (1.01)
0.0	1.0	6.84m (1.01)	33037ton (0.97)
Reference model		6.75m (1.00)	33934ton (1.00)

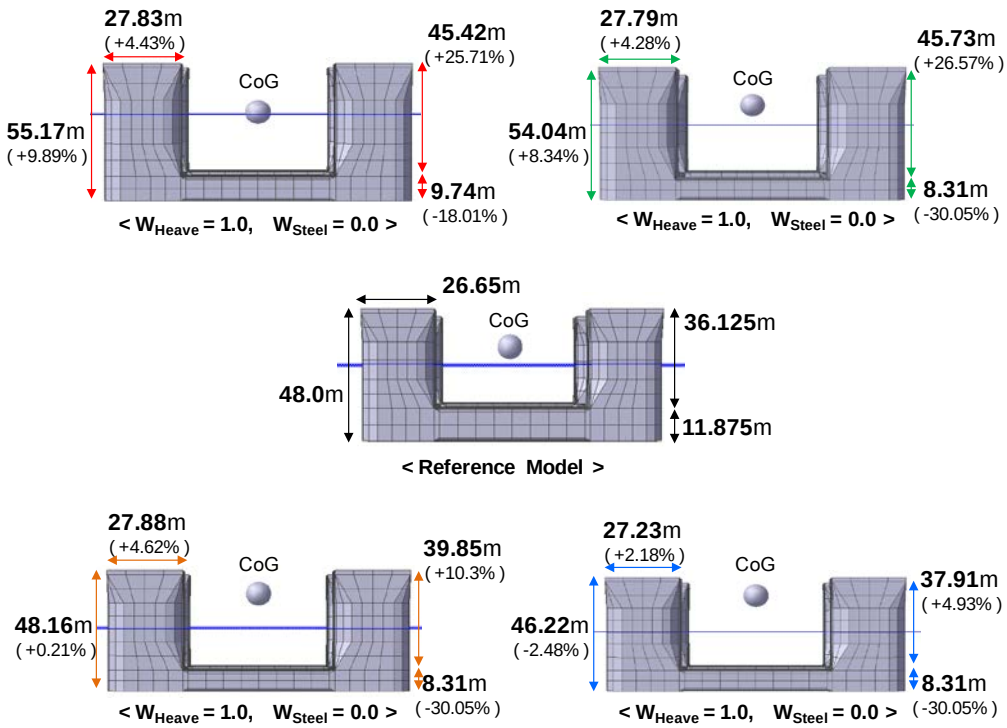

Fig. 27 – Hull form of the optimal solutions

Table 11 – Constraints of the optimal solutions

W_H	W_W	GM	Min. Air gap	Total Height	Draught	Freeboard
1.0	0.0	9.64m	2.01m	55.17m	34.77m	20.40m
0.5	0.5	9.16m	2.29m	54.04m	30.54m	23.50m
0.2	0.8	11.82m	3.78m	48.16m	25.08m	23.08m
0.0	1.0	11.14m	2.72m	46.22m	24.22m	22.00m
Ref.		7.98m	−0.06m	48.00m	27.62m	20.38m

Fig. 27 shows the hull form of the optimal solutions and Table 11 shows the constraints of each solution. As the weighting factor of steel weight is increased, total height decreases so that the resultant weight decreases. On the other hand, heave response deteriorates with the increase of same weighting factor. This can be explained by Fig. 28, 29.

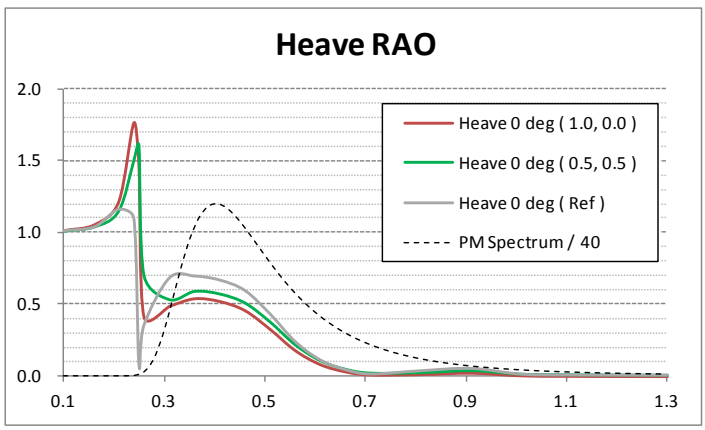

Fig. 28 – Heave RAO of two cases corresponding to high W_{Heave}

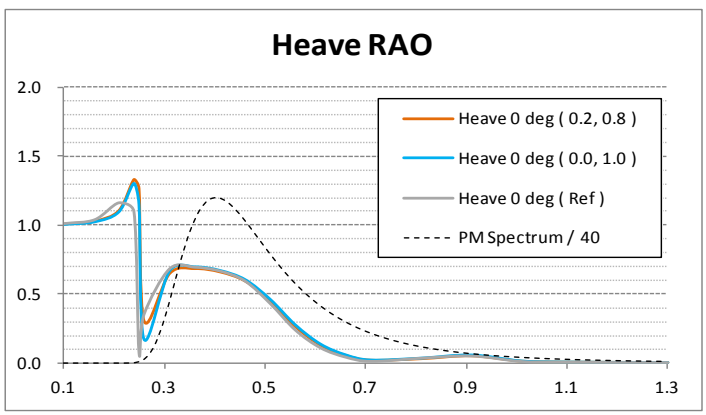

Fig. 29 – Heave RAO of two cases corresponding to low W_{Heave}

When the weighting factor of heave motion is relatively large, the second peak of heave motion RAO is much smaller than the of the reference model. However, the weighting factor of steel weight is relatively large, the second peak of heave RAO is not much different from the reference model.

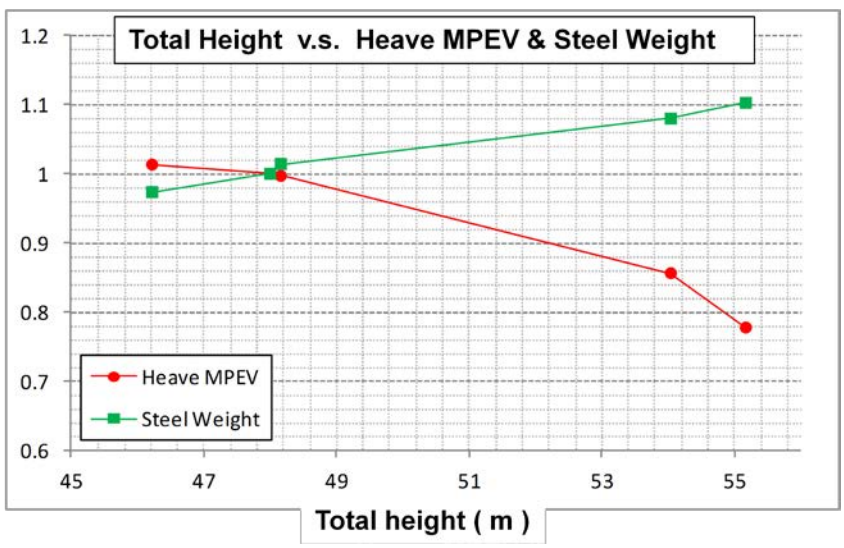

Fig. 30 – Tendency between total height and heave response, steel weight

Fig. 30 shows the tendency between total height and heave response, steel weight. It is found that total height is in proportion to steel weight and inverse proportion to heave response.

4. Conclusion

In this study, the hull form of semi-FPU is optimized. The object is to minimize heave motion response and to minimize steel weight. GM is considered as a constraint for the stability. Additionally air gap is required to be greater than 2.0m to avoid the risk of bottom slamming which can cause a structural failure of topside.

As a preparatory work for the optimization, three modules are introduced. In panel generation module, ten geometric parameters defined. Using B-spline and Bezier surface method, the geometry is represented, mesh is generated consequently. In mass estimation module, weight and CoG are estimated based on the surface area, the volume and the other dimensions of hull. In conditions setting module, the condition for the motion analysis and the air gap analysis which will be used in WADAM are set.

Using simulated annealing algorithm, four optimal solutions are obtained. The solutions are from different weighting factors and they are identified to be reasonable by the comparison of each other. As increasing the preference of steel weight, steel weight decreases due to the shortened column height, but leads to worse

heave motion performance. It is found that heave response is in inverse proportion to total height.

The estimation method of steel weight needs to be improved. The present method estimates the steel weight just by means of the surface area. This method is based on the assumption that the thickness of outer plates is uniform. However, the real structure is not uniform that the thickness of the plate differs according to the global forces such as the split force and the torsion moment. So the new method should be able to consider the global forces.

The optimization algorithm also needs to be improved. In the present one, the number of iteration, 400, is the only convergence criteria. But it cannot be guaranteed that 400 times of iteration is sufficient or not. Actually some results seemed to have room for more decrease. So the new criteria which can judge whether to proceed or not by the objective values.

It is expected that the procedure introduced in this study can be used as a standard in the early design stage. Not only semi-submersible type but also other offshore structures can be modified to have better performances; leads to the economical advantage.

Reference

[1] Akagi, S., Ito, K., "Optimal Design of Semisubmersible Form by Minimizing its Motion in Random Seas", *Journal of Mechanisms, Transmissions and Automation in Design* , Vol.106, pp.23-30, 1984.

[2] Akagi, S., Yokoyama, R., Ito, K., "Optimal Design of Semisubmersible's Form Based on System Analysis", *Journal of Mechanisms, Transmissions and Automation in Design* , Vol.106, pp.524-530, 1984.

[3] Lee, J. Y., Clauss, G.F., "Automated Development of Floating Offshore Structures in Deepwater with Verified Global Performances by Coupled Analysis", *Proceedings of the 17th International Offshore and Polar Engineering Conference* (ISOPE), Lisbon, Portugal, 2007.

[4] Rao, S. S., "Engineering Optimization: Theory and Practice", 3rd edition, New Age International, 1996.

[5] Rogers, D. F., "An Introduction to NURBS with Historical Perspective", Morgan Kaufmann Publishers, 2001.

국문 초록

운동성능과 구조중량을 고려한 반잠수식 FPU의 하부구조 형상최적화에 관한 연구

본 논문에서는 실재 반잠수식 FPU(Floating Production Unit)의 하부구조를 대상으로 수직운동과 구조중량이 최소가 되는 최적의 형상을 결정하였다.

심해 유전 개발이 활발히 이루어짐에 따라, 부유식 해양구조물에 대한 수요가 늘어나고 있다. 부유식 구조물은 거친 해상 상태에서 큰 수직운동을 동반하며, 이로 인하여 상부구조의 생산활동이 불가능한 다운타임이 발생하게 된다. 이러한 다운타임을 줄이는 것은 경제성과 직결되므로, 작은 수선면적으로 인해 비교적 높은 운동성능을 보이는 반잠수식 구조물이 선호되고 있다.

파랑하중에 의한 운동의 변위는 하부구조의 형상과 밀접하게 연관되어 있으므로, 반잠수식 구조물의 장점을 극대화하기 위해서는 하부구조의 최적형상을 결정하는 것이 필수적이다. 위와 같은 이유로 본 논문에서는 반잠수식 FPU의 하부구조 형상 최적화를 위한 자동화된 절차를 소개하였으며, 실재 구조물을 대상으로 최적화를 수행하였다.

운동성능해석에는 상용 소프트웨어인 DNV WADAM을 이용하였다. WADAM은 두 가지의 입력파일을 필요로 하는데, 최적화가 과정에서 자동으로 두 파일을 생성하기 위한 세 가지 모듈이 개발되었다.

Panel generation module은 하부구조를 열 개의 부분으로 나누어, 각 부분의 제원에 해당하는 열 가지 매개변수를 정의하여 하부구조의 형상을 표현한다. 기하학적 형상을 정의하기 위하여 B-spline 곡면을 이용하고, 광역 격자 크기(global mesh size)에 따라 등 간격으로 격자를 생성한다.

Mass estimation module은 전체 구조물의 중량과 무게중심을 추정한다. 중량과 무게중심은 상부구조 중량, 강재 중량, 의장 중량, 밸러스트 수 중량 그리고 기타 항목으로 나누어 추정하며, 각 항목의 추정은 하부구조의 표면적과 체적 및 기타 제원을 기반으로 한다.

Conditions setting module은 주파수, 파 선수각, 해상상태와 같은 해석조건을 설정한다. 본 연구에서는 슬래밍에 의한 상부구조의 파괴를 방지하기 위하여 air gap 해석을 추가적으로 수행하는데, air gap을 확인하기 위한 53개의 점이 이 모듈에서 지정된다.

최적화의 알고리즘으로는 모의 담금질 기법(simulated annealing)을 이용하였다. 열 가지의 형상 매개변수 중 세 가지 주요 제원을 선택하였고, 유동적인 밸러스트 수의 양을 제어하기 위한 변수를 더하여 총 네 가지의 설계변수가 정의되었다. 제약조건으로 GM, 최소 air gap, 건현,

흘수, 하부구조의 전체 높이가 고려되었으며 상부구조의 지지를 위하여 컬럼 사이의 거리는 일정하게 유지되었다.

상하동요 운동응답(heave response) 최소화, 구조 중량 최소화의 두 가지 목적에 대한 선호도를 조절하는 가중인수(weighting factor)를 도입하여, 선호도 차이에 따른 네 개의 최적 해를 도출하였다. 구조 중량에 대한 선호도가 증가함에 따라 하부구조의 전체 높이가 줄어들며, 이로 인해 구조 중량이 감소하지만, 운동성능은 더욱 나빠짐을 확인할 수 있었다. 또한 전체 높이와 상하동요 운동응답 사이에는 반비례관계가 있음을 확인할 수 있었다.

키워드: 반잠수식 FPU, B-spline 곡면, 상하동요 운동 응답, 구조 중량, 형상 최적화, 모의 담금질 기법

학번: 2011-23462